

Electronic Supplementary Information

for

Self-assembled, nanostructured coatings for water oxidation by alternating deposition of Cu-branched peptide electrocatalysts and polyelectrolytes

*Enikő Farkas,^a Dávid Srankó,^b Zsolt Kerner,^b Bartosz Setner,^c Zbigniew Szewczuk,^c Wiesław Malinka,^d Robert Horvath,^{*a} Łukasz Szyrwiel^{*d,e} József S. Pap^{*b}*

^aNanobiosensorics Group, MTA Centre for Energy Research - MFA, H-1121 Budapest, Hungary. E-mail: horvathr@mfa.kfki.hu

^bSurface Chemistry and Catalysis Department, MTA Centre for Energy Research, H-1121 Budapest, Konkoly Thege str. 29-33, Hungary. E-mail: pap.jozsef@energia.mta.hu

^cFaculty of Chemistry, Univ. of Wrocław, ul. F. Joliot-Curie 14, 50-383 Wrocław, Poland

^dDept. of Chemistry of Drugs, Wrocław Medical Univ., ul. Borowska 211, 50-552 Wrocław, Poland. E-mail: lukszyr@wp.pl

^eCNRS/UPPA, LCABIE, UMR5254, Helioparc, 2, av. Pr. Angot, F-64053 Pau, France

Contents:

Table S1.

X-ray photoelectron spectroscopy (XPS) on LbL-ITO with **Cu-3G** and PLL.

Figs. S1-S20.

Table S1. XPS surface composition of LbL-ITO made with 20 deposition cycles of **Cu-3G** and PLL.^a

elements / component peak	Binding energy (eV)	Chemical states	Surface conc. (at.%)
Cu 2p	933.1	Cu(I)	3.1
O 1s	530.3	Oxides	13.5
	530.8	Oxides, hydroxides, PO ₄ ³⁻	16.4
	531.7	O=C	3.8
	532.9	O-C	2.5
Sn 3d	486.3	SnO, SnO ₂	0.3
In 3d	444.0	In ₂ O ₃	3.9
N 1s	400.0	peptide, amine	8.8
N 1s	401.3	alkylammonium ion	2.3
C 1s	284.8	C-C, C-H	21.7
	286.0	C-O, C-N, C=N	10.7
	287.8	C=O, peptide	7.6
	290.1	O-C=O	0.2
	291.4	π - π^* satellite	0.2
P 2p	132.5	PO ₄ ³⁻	2.1

^aconditions of deposition were identical to those of Fig. 1A, 0.5 mM bulk **Cu-3G** concentration was applied, the final cycle was that of the Cu complex followed by rinse

X-ray photoelectron spectroscopy (XPS) on LbL-ITO with Cu-3G and PLL. The very low ratio of the metals associated with ITO and the oxygen content [(Sn+In)/O = 0.12]

indicates the presence of further compounds on the surface in considerable density. The binding energy of the *Sn 3d* and *In 3d* peaks were assigned to their oxides (*Sn 3d*_{5/2} = 486.3 eV and *In 3d*_{5/2} = 444.0 eV) and the surface modification did not cause any changes in their chemical states.

There is high carbon content on the surface as would be expected for a PLL coating. The peak at 284.8 eV is related to the C-C/C-H bonds (Fig. S1A). The peak at 286.0 eV is typical for carbon in C-O as well as for C-N and C=N bonds,^{S1-S3} while the 287.8 eV peak can be assigned to the carbon in C=O bonds of amide groups.^{S1-S3} A small (barely detected) C 1s peak appears at 290.1 eV that may indicate the presence of some O-C=O groups. The copper content was determined both by the presence of *Cu 2p* (Fig. S1B) and by the *Cu LMM* peaks (Fig. S2). The *Cu 2p* peak is observed at 933.1 eV while the position of the *Cu 2p*_{3/2} and a slightly visible shake up peak is at ~942 eV. These are typical for the Cu(I) state,^{S4} however Cu(II) is known to be sensitive of the reductive environment of ultra-high vacuum conditions. For a better understanding of the chemical environment of copper, the modified Auger parameter was calculated using the following formula: $\alpha' = E_k(C_1C_2C_3) + E_b(C)$, where $E_k(C_1C_2C_3)$ is the kinetic energy of the Auger transition involving electrons from C₁, C₂ and C₃ core levels and $E_b(C)$ is the binding energy of the core level C.^{S5} The $\alpha' = 1846.6$ eV value is typical for the copper in organic environment in the presence of nitrogen,^{S6} and thus confirms the presence of Cu bound by peptide nitrogen atoms (see also ref. 34).

The majority of the oxygen content originates from inorganic compounds such as oxides, hydroxides or phosphates (Fig. S1C). The oxides and hydroxides are components of the ITO substrate, while phosphate is built into the film from the buffer solution in accordance with OWLS findings. Supporting, a peak appears at 132.5 eV characteristic for *P 1p* and *2p* in phosphate (Fig. S3). This value corroborates the presence of phosphate and clearly attributes some of the oxygen at 530.8 eV to the phosphate.^{S7} The presence of P in the composite can be attributed to H₂PO₄⁻/HPO₄²⁻ counter ions coupled to PLL terminal ammonium groups (see the corresponding N/P ratio of 2.3/2.1). This sort of interaction is known to facilitate the binding of lysine containing metalloproteins to the phosphate units of DNA (see ref. 42).

The *O 1s* peaks appearing at higher binding energies can be assigned to the oxygen in organic compounds. The *O 1s* at 531.7 eV is a characteristic for the O=C bond and the 532.9 eV signal is ascribed to O-C bonds.^{S7} Nitrogen content was detected at peak energies that are typical for an organic environment (Fig. S1D). The peaks at 400.0 eV and 401.3 eV are assigned to the *N 1s*, the minor peak at higher binding energy (401.3 eV) is typical for the

alkyl ammonium ions^{S8} confirming that lysine terminal amines of PLL are in part protonated. Altogether these results indicate that LbL buildup among the above conditions leads to saturation of anchoring sites at PLL with the increasing number of complex additions.

References

- (S1) Truica-Marasescu, F.; Wertheimer, M. R. *Plasma Proc. Polym.* **2008**, *5*, 44-57.
- (S2) Briggs, D.; Brewis, D. M.; Dahm, R. H.; Fletcher, I. W. *Surf. Interface Anal.* **2003**, *35*, 156-167.
- (S3) Shard, A. G.; Whittle, J. D.; Beck, A. J.; Brookes, P. N.; Bullett, N. A.; Talib, R. A.; Mistry, A.; Barton, D.; McArthur, S. L. *J. Phys. Chem. B* **2004**, *108*, 12472-12480.
- (S4) Wagner, C. D.; Naumkin, A. V.; Kraut-Vass, A.; Allison, J. W.; Powell, C. J.; Rumble Jr., J. R. *NIST Standard Reference Database 20*, Version 3.4 (web version) (<http://srdata.nist.gov/xps/>) **2003**.
- (S5) Gaarenstroom, S. W.; Winograd, N. *J. Chem. Phys.* **1977**, *67*, 3500-3506.
- (S6) Arkhipushkin, I. A.; Yu. E. Pronin, Vesely, S. S.; Kazansky, L. P. *Int. J. Corros. Scale Inhib.* **2014**, *3*, 78-88.
- (S7) Moulder, J. F.; Stickle, W. F.; Sobol, P. E.; Bomben, K. D. *Handbook of X-ray Photoelectron Spectroscopy*, Perkin-Elmer Corp., Eden Prairie, MN, **1992**.
- (S8) Beamson, G.; Briggs, D. *High Resolution XPS of Organic Polymers - The Scienta ESCA300 Database*, Wiley Interscience, **1992**.

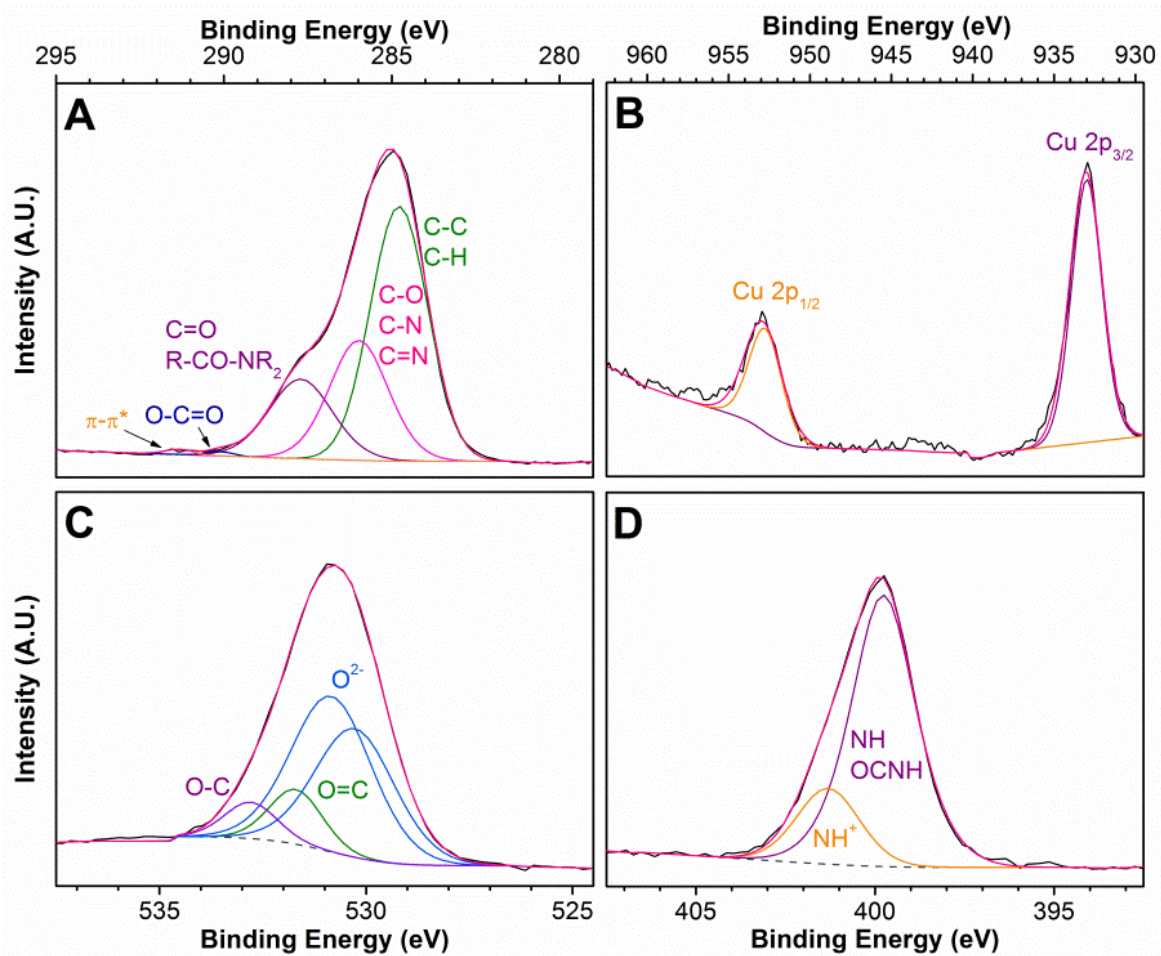


Figure S1. Recorded and fitted XP spectra of (A) C 1s, (B) Cu 2p, (C) O 1s and (D) N 1s measured on ITO after 20 deposition cycles of **Cu-3G** and PLL (for data see Table 1, pH = 7.5, 0.5 mM bulk **Cu-3G** concentration, the final cycle of deposition is that of Cu complex).

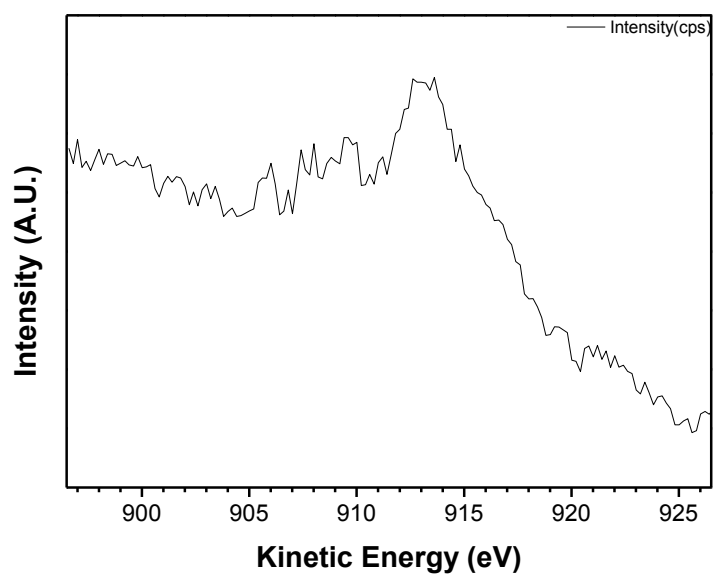


Figure S2. XP spectrum of Cu LMM.

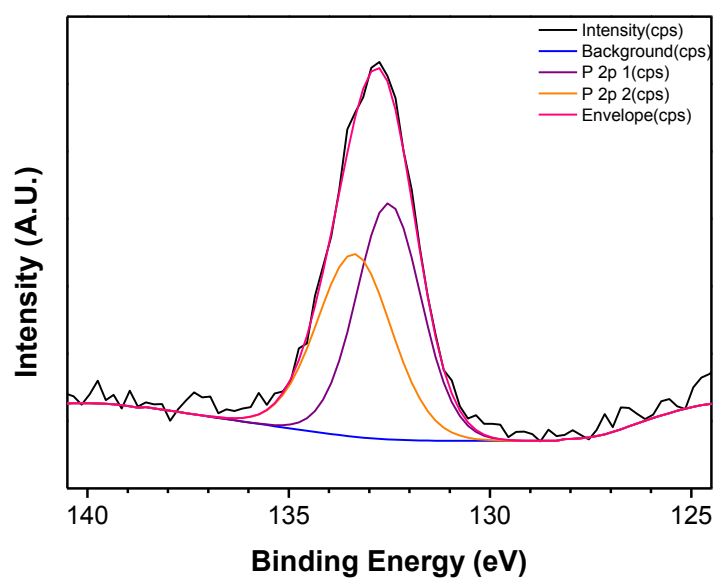


Figure S3. XP spectra part of P $2p_{1/2}$ and $2p_{3/2}$, at energies that are typical for phosphate.

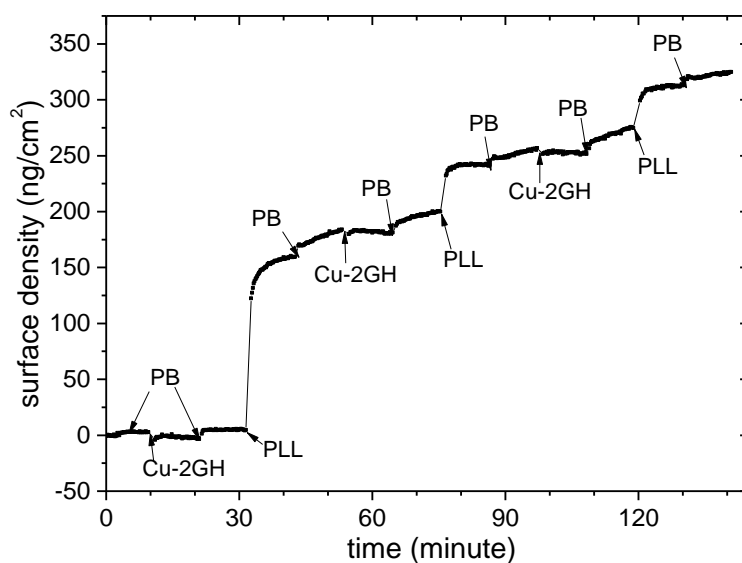


Figure S4. Deposition attempt with PLL and Cu-2GH (0.5 mM) on ITO coated chip in 0.1 M PB at pH 7.5.

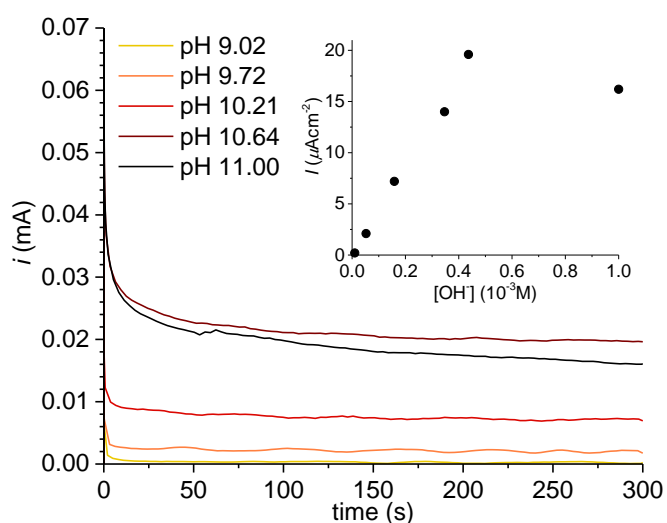


Figure S5. Controlled potential electrolysis (CPE) on LbL-ITO electrodes after 8 deposition cycles of Cu-3G/PLL/phosphate, performed at 1.1 V vs. Ag/AgCl, in 0.1 M phosphate at the indicated pH values. All CPE experiments were preceded by a 3-cycle CV scan from 0 to 1.2 V. The corresponding CVs are shown in Fig. 3. Inset: current values at the end of the 5 min CPE experiment plotted as a function of $[\text{OH}^-]$.

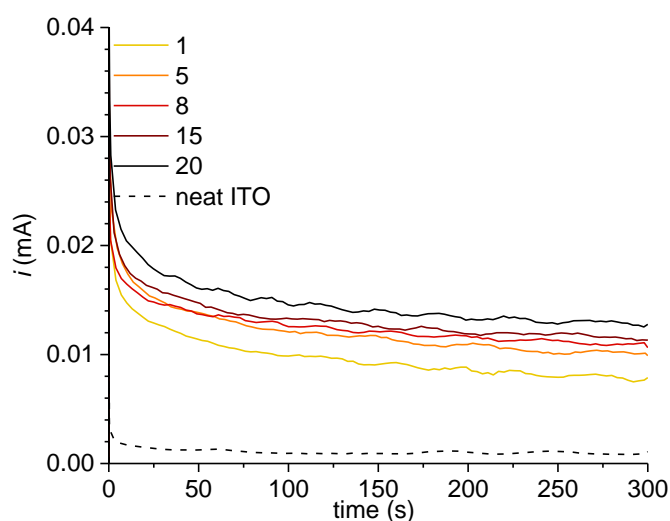


Figure S6. CPE on LbL-ITO electrodes treated with various numbers of deposition cycles (as indicated in the legend) of **Cu-3G/PLL/phosphate** in solutions containing 0.1 M phosphate (pH = 10.55) at 1.1 V vs. Ag/AgCl. All CPE experiments were preceded by a 3-cycle CV scan from 0 to 1.2 V. Some corresponding CV experiments are plotted and explained in Fig. S8.

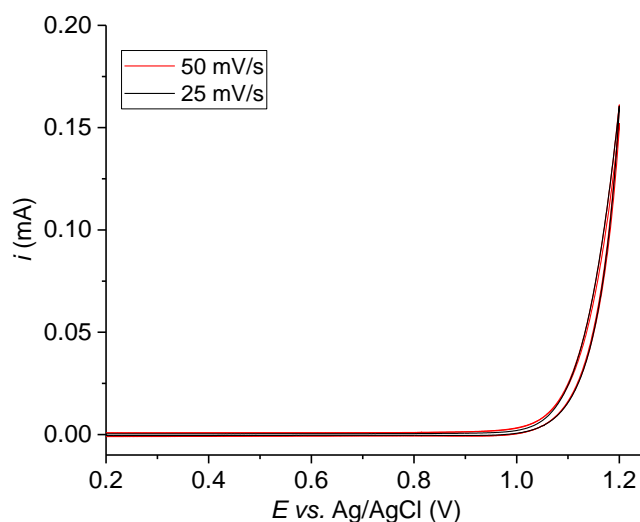


Figure S7. CVs on LbL-ITO electrode treated with 20 deposition cycles of **Cu-3G/PLL/phosphate** (pH = 10) at 50 (red) and 25 mV/s (black) scan rate in 0.1 M phosphate solution at pH = 10.6. The scans were recorded after 10 minutes of CPE at 1.1 V.

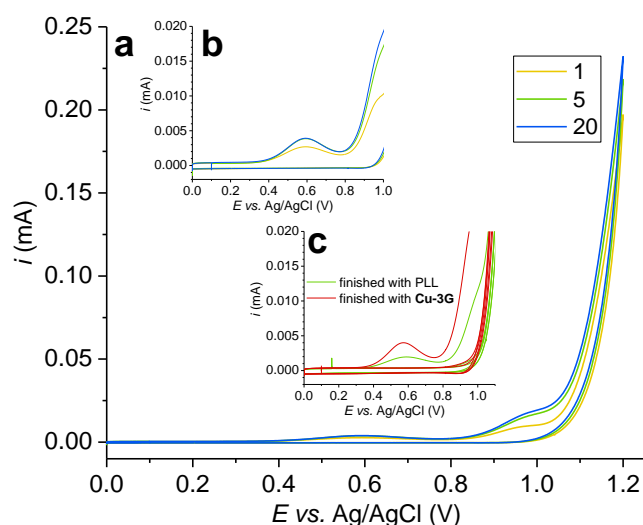


Figure S8. (a) First cycles of CVs on LbL-ITO electrodes with the indicated, increasing number of **Cu-3G**/PLL/buffer deposition cycles (pH = 10), at 25 mV/s scan rate, in 0.1 M phosphate solution at pH = 10.55; (b) blown up picture of the current peak attributed to the **Cu-3G** that leaves upon further polarization and plays no role in the course of CPE (note that this Cu(III/II) peak shows saturation above deposition cycle number of 5); (c) comparison of CVs (3 cycles) on ITO deposited with 8 **Cu-3G**/PLL/phosphate cycles, finished with PLL (green) or **Cu-3G** (red). The ratio of the Cu(III)/Cu(II) peaks indicates that the affected fraction of complex should correspond to the amount deposited in ~2-3 cycles. Quantitative analysis of this peak according to equation: $i_p = n^2 F^2 A \Gamma^0 \nu / 4RT$, where i_p is the peak potential (corrected with capacitive current, n is the number of electrons, F is the Faraday constant, $A \sim 1 \text{ cm}^2$ and $\nu = 0.025 \text{ V/s}$. Γ^0 thus can be calculated as $0.65 \times 10^{-10} \text{ mol/cm}^2$ (finished with PLL, green curve) and $1.49 \times 10^{-10} \text{ mol/cm}^2$ (coating finished with **Cu-3G**, red curve). The numbers should be compared to the value of $3.96 \times 10^{-10} \text{ mol/cm}^2$ (8 deposition cycles) calculated from OWLS in Table 2.

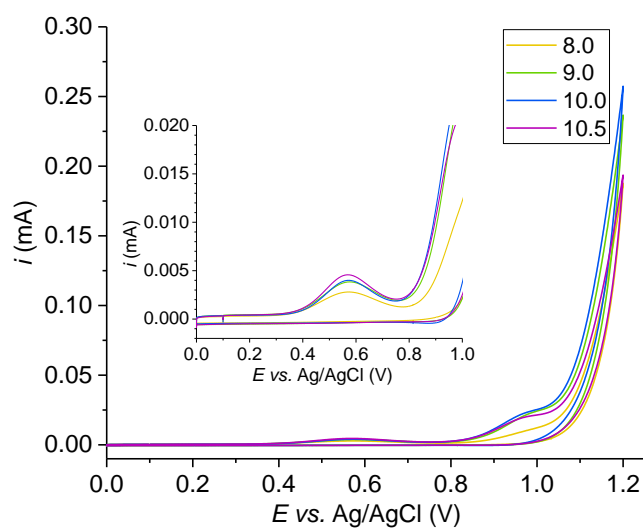


Figure S9. Effect of pH on deposition. First cycle of CVs on LbL-ITO electrodes after 8 deposition cycles of **Cu-3G/PLL/phosphate** at different pH values (as indicated), at 25 mV/s scan rate. The CVs were taken in 0.1 M phosphate solution at pH = 10.64. Inset: blown up picture of the current peak attributed to the surface bound **Cu-3G** that transforms non-reversibly upon polarization and in its original form plays no further role in sustained electrolysis.

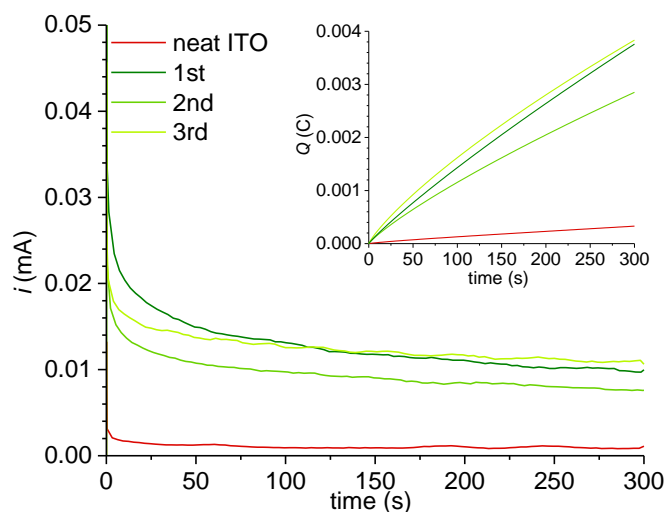


Figure S10. Controlled potential electrolysis (CPE) on ITO electrode with or without **Cu-3G/PLL/phosphate** coating in a solution containing 0.1 M phosphate (pH = 10.55). The green lines represent 1st, 2nd and 3rd round of 5 minutes long polarization at 1.1 V vs. Ag/AgCl, which were performed by placing the electrode into a new electrolyte each time. Inset: blown

up picture of the charge transport. All CPE experiments were preceded by a 3-cycle CV scan from 0 to 1.2 V.

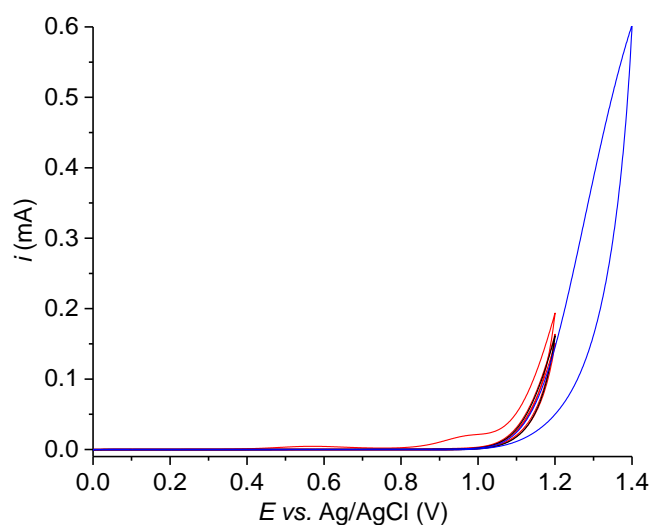


Figure S11. First 3 cycles of CV scans at 25 mV/s scan rate on LbL-ITO electrode treated with 8 deposition cycles of **Cu-3G**/PLL/phosphate (pH = 10.5, red). The same electrode was exposed to 10 minutes of CPE at 1.1 V and scanned again to 1.2 V (black) three times and up to 1.4 V (blue) in 0.1 M phosphate solution at pH = 10.6.

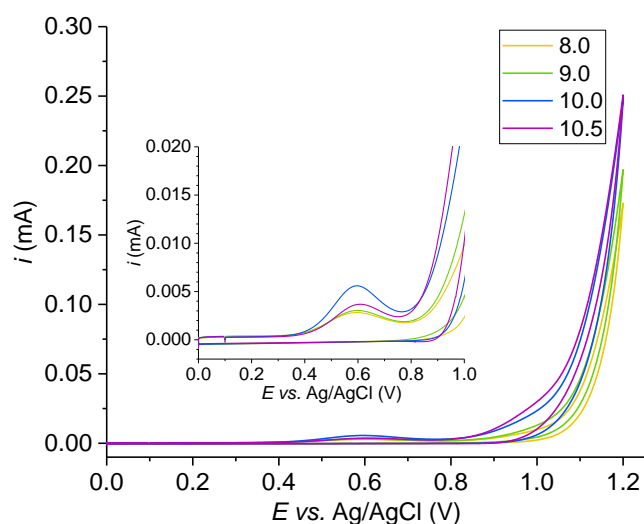


Figure S12. The effect of pH on deposition. First cycle of CVs on LbL-ITO electrodes treated with 8 deposition cycles of **Cu-2GH**/PAH/phosphate at various pH values, taken at 25 mV/s scan rate. The CVs were recorded in 0.1 M phosphate solution at pH = 10.55. Inset: blown up view of the current peak attributed to the Cu(III/II) transition of **Cu-2GH**.

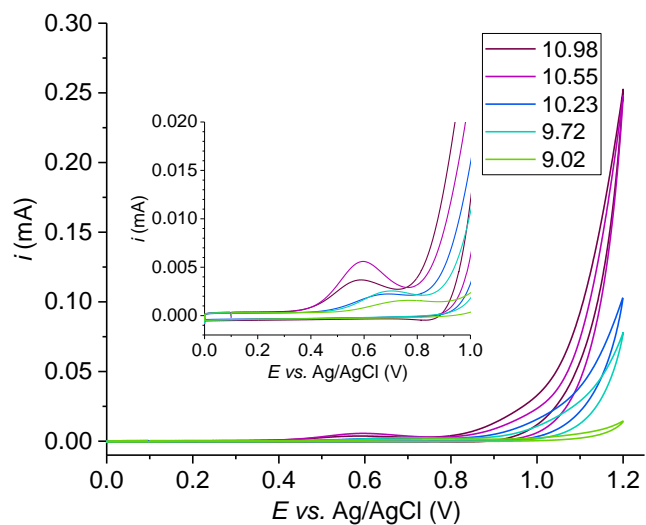


Figure S13. First cycle of CV scans on LbL-ITO deposited 8 times with **Cu-2GH/PAH/phosphate** (at pH = 10) in 0.1 M phosphate solution at different pH values as indicated; inset: blown up picture of the current peak attributed to the portion of **Cu-2GH** undergoing non-reversible transformation. Scan rates were 25 mV/s uniformly.

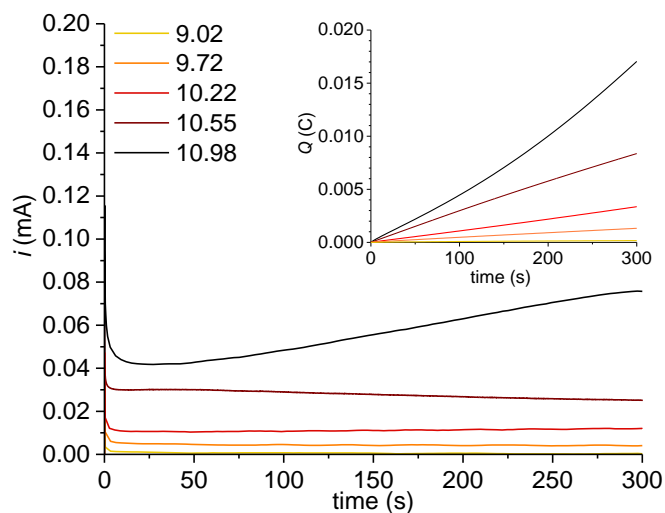


Figure S14. Controlled potential electrolysis (CPE) on LbL-ITO electrodes deposited 8 times with **Cu-2GH/PAH/phosphate**, performed at 1.1 V vs. Ag/AgCl in 0.1 M phosphate electrolyte at the indicated pH values. All CPE experiments were preceded by a 3-cycle CV scan from 0 to 1.2 V. The corresponding CVs are shown in Fig. S13.

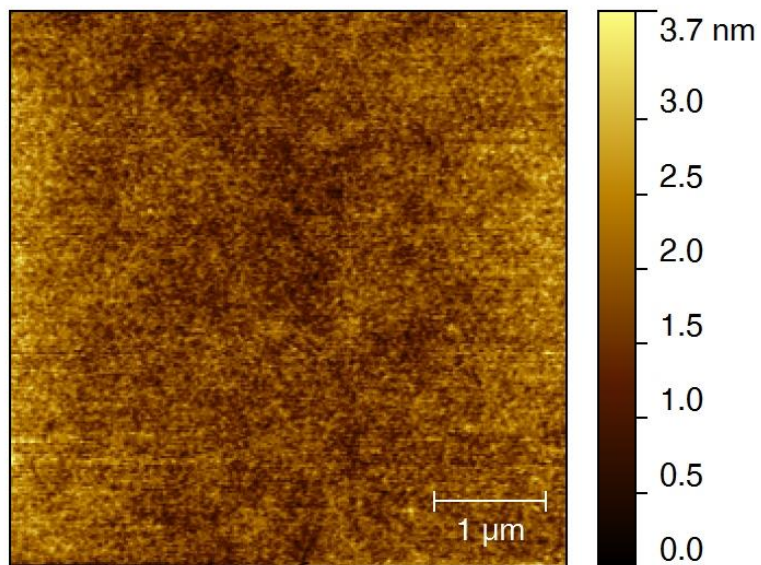


Figure S15. Representative AFM image of the bare ITO chip surface ($5 \times 5 \mu\text{m}$).

Foot-of-the-wave analysis (FOWA). FOWA renders catalytic current to the activated proportion of the catalyst generated by polarization of the electrode according to eq. (1),

$$i = \frac{nFA\Gamma_{cat}^0 k[S]}{1 + e^{\frac{F}{RT}(E_{cat}^0 - E)}} \quad (1)$$

, where $n = 4$ is the number of electrons, F is the Faraday constant, A is the surface area of the electrode ($\sim 1 \text{ cm}^2$), Γ_{cat}^0 is the surface density of the catalyst (mol/cm^2), $[S]$ is the substrate concentration (M), $k_{cat} = k[S]$ is the apparent rate constant (s^{-1}) and E_{cat}^0 is the formal potential of the redox step triggering catalysis.

This method allows the estimation of TOF reflecting the intrinsic chemical properties of the catalyst regardless of influencing side phenomena that may occur typically at higher polarization of the electrode or extreme pH *e.g.* product inhibition and deactivation or decomposition of the catalyst. For the optimization of complex systems, where the thermodynamic driving force (high pH and anodic polarization of the electrode) for efficient catalysis and detrimental side phenomena (such as the degradation of organic compounds) may strongly overlap, FOWA can be useful to obtain rate constants descriptive of the relatively unperturbed system. In the case of our systems it is relevant, since pH has been demonstrated to drive Cu:ligand equilibrium systems in water oxidation electrocatalysis either toward heterogeneous film deposition, or operating as a homogeneous system.¹⁹

In the present study the aim was to find conditions where the systems are sustained in a state that allows the catalyst molecules remaining linked with the polyelectrolyte at the electrode surface and degradation is not yet a significant factor. According to the FOWA method, eq. (1) was applied to analyse CV curves.

For the successful application of FOWA two parameters, Γ_{cat}^0 and E_{cat}^0 had to be determined first. The surface density could be estimated from OWLS data (Fig. 1, see Table S2) and E_{cat}^0 from square wave voltammetry (SWV) experiments. SWV on ITO pieces layered with **Cu-3G/PLL/phosphate** or **Cu-2GH/PAH/phosphate** was performed at pH = 10.55 (Fig. S16) in 0.1 M NaClO₄ electrolyte (phosphate was only present within the surface film). The **Cu-3G/PLL** combination showed current peak at 1.12 V, whereas the **Cu-2GH/PAH** signal appears at ~ 1.14 V (as shoulder), both sitting on top of an increasing current wave. These potential values can be associated with an altered complex form (see mechanism proposal and cycle B in Scheme 5) and correspondingly, with E_{cat}^0 that is applied in FOWA as the oxidative transition

triggering the catalytic event (note that k_{cat} values stand for cycle B of the proposed mechanism, because the initial processes that precede sustainable electrolysis do not participate in it).

Note that the k_{cat} value of 8.36 s^{-1} at $\text{pH} = 10.98$ lags behind that for the homogeneous system for **Cu-2GH**. In part this can be attributed to the difference between GCE and ITO (previous studies mention that catalysis can be 8 times faster at GCE than at ITO,¹⁸ but according to our experimental findings the difference is rather due to a shift in the mechanism in the presence of polyelectrolyte (Scheme 5).

Table S2. Apparent rate constant (k_{cat} , s^{-1}) derived by FOWA of CV curves taken by using LbL-ITO working electrodes with **Cu-3G/PLL** or **Cu-2GH/PAH** films.^a

electrolyte pH	LbL deposition cycles	slope (error in last digit)	Γ_{cat}^0 ($10^{-10} \text{ mol/cm}^2$)	$k_{cat}(\text{Cu-2GH})/k_{cat}(\text{Cu-3G})$ ratio
Cu-3G/PLL				
10.55	1	1.48(1)	0.88	
10.55	5	1.11(1)	2.64	
10.55	8	1.09(1)	3.96	
10.55	15	0.29(1)	7.02	
10.55	20	0.35(1)	9.24	
Cu-2GH/PAH				
10.55	1	3.63(2)	0.72	2.45
10.55	5	1.54(1)	2.15	1.39
10.55	8	2.87(2)	3.24	2.63
10.55	15	0.82(1)	5.73	2.82
10.98	8	8.36(7)	3.24	

^adeposited at $\text{pH} = 10$ (0.1 M PB, 0.5 mM bulk complex concentration, the final deposition is that of the Cu complex in each case), immersed into 0.1 M PB, at 25 mV/s scan rate, the number of **Cu-3G** deposition cycles is always one more than the indicated number of LbL deposition cycles and Γ_{cat}^0 is calculated accordingly.

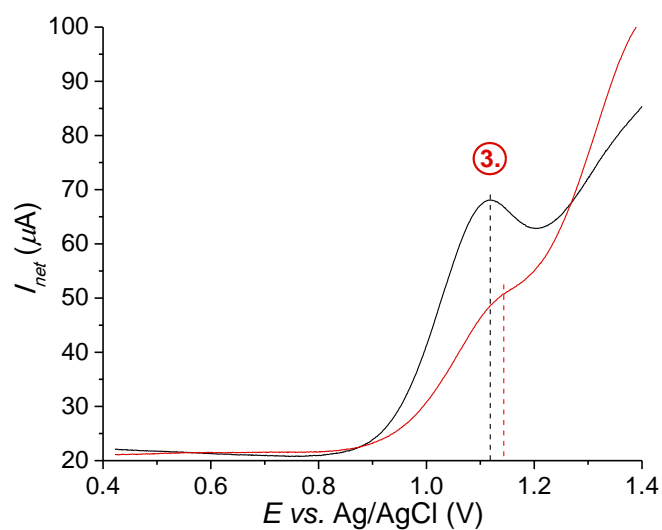


Figure S16. Current peaks detected by SWV at pH = 10.55 in 0.1 M NaClO₄ electrolyte for LbL-ITO electrodes layered with **Cu-3G/PLL** (black) and **Cu-2GH/PAH** (red). The E_{net} potentials are associated with the catalysis triggering event (E_{cat}^0) and the values have been used for FOWA. The corresponding step in the proposed mechanism is identified with a circled red number in Scheme 5 and here, too.

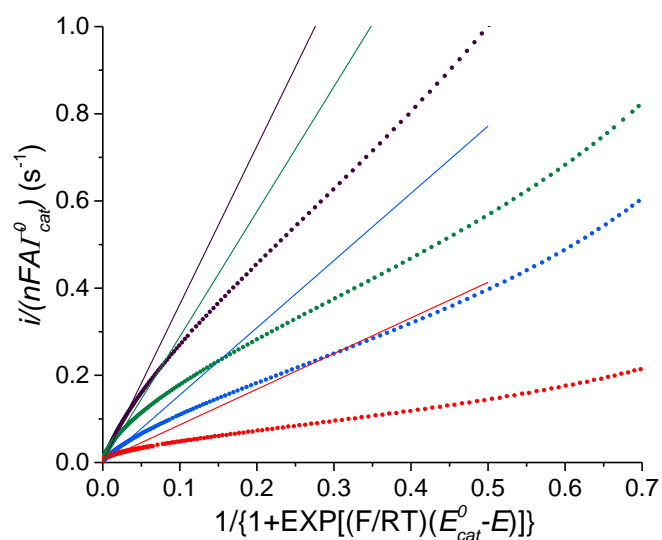
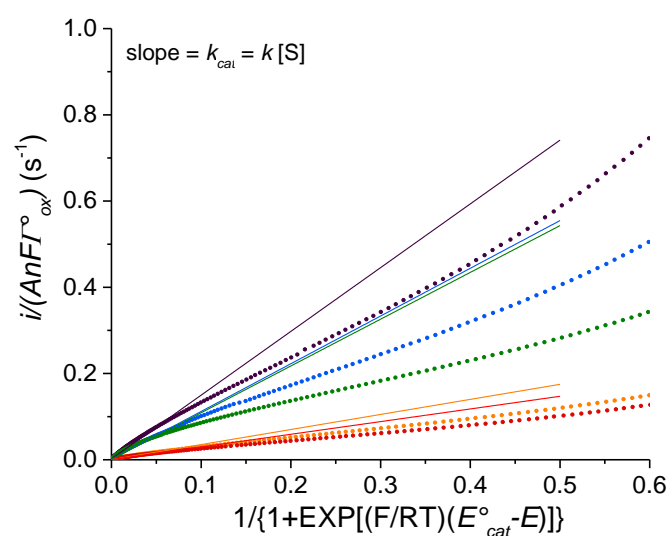


Figure S17. Top: FOWA of anodic direction of CV datasets for the **Cu-3G/PLL/phosphate** system built with increasing number of deposition cycles (orange: 20, red: 15, green: 8, blue: 5, purple: 1). Associated data and conditions are found in Table S2. Bottom: the same analysis for the **Cu-2GH/PAH/phosphate** system built with increasing number of deposition cycles (orange: 15, red: 8, green: 5, blue: 1). Associated data and conditions are indicated in Table

S2.

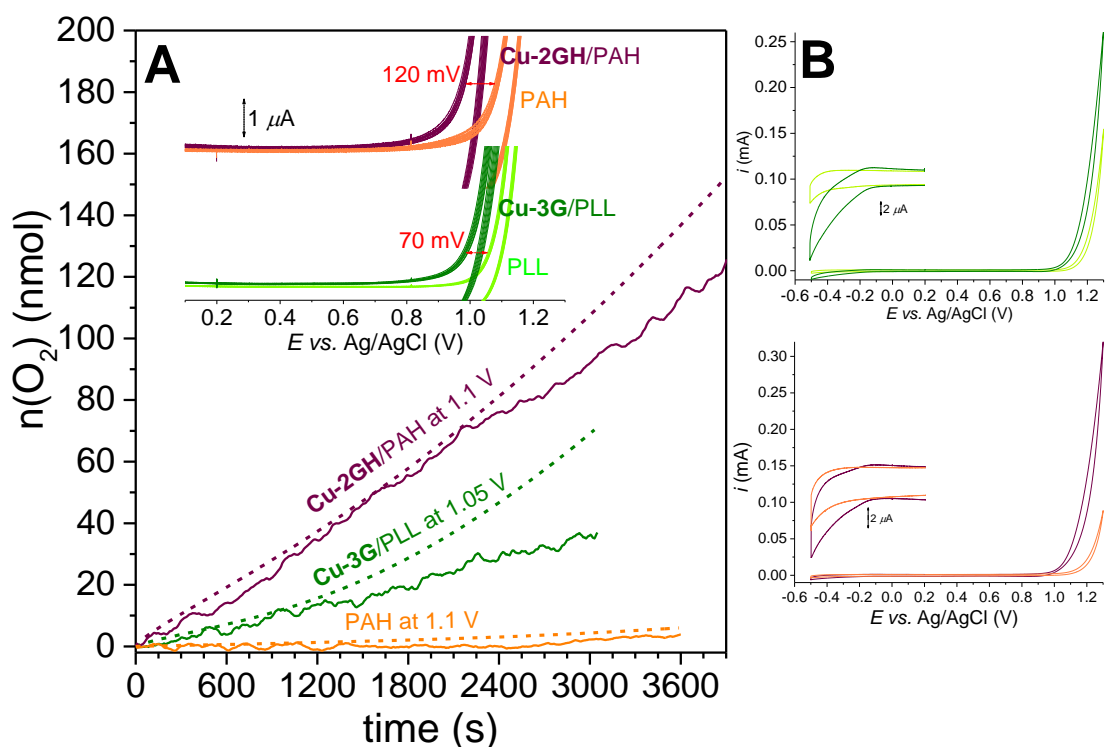


Figure S18. (A) O_2 production detected by fluorescence probe immersed into the electrolyte (solid lines) in the course of CPE among the indicated conditions and the amount of O_2 calculated from charge (dashed lines) for **Cu-3G/PLL/phosphate**, **Cu-2GH/PAH/phosphate** and **PAH/phosphate** (8 deposition cycles each at $\text{pH} = 10$) on ITO at $\text{pH} = 10.6$ in 0.1 M phosphate electrolyte at 25°C (stirring was applied, PLL/phosphate behaves very similarly to PAH/phosphate). Faradaic efficiency is high up to 1200 s (roughly 30 turnovers) and 2400 s (roughly 230 turnovers) for **Cu-3G/PLL/phosphate** and **Cu-2GH/PAH/phosphate**, respectively, deposited amounts of complexes were considered as given in Table S2. Inset: blown-up view of 10 CV scans from -0.5 to 1.3 V (current scale is 0 to 4 μA) on the LbL-ITO electrodes used in CPE (colours render the CVs to the corresponding O_2 curves, *i.e.* CPE experiments of the main figure). The potential values in red stand for the approximate difference between the onset potential of the catalytic current and the oxidation current with polyelectrolyte-only coating. (B) Representative CV scans for both systems (colours are the same as previously) and blown-up view of a reduction feature characteristic for Cu-complex content and missing from polyelectrolytes. On the basis of its position it can be associated with a Cu(II)/Cu(I) transition.

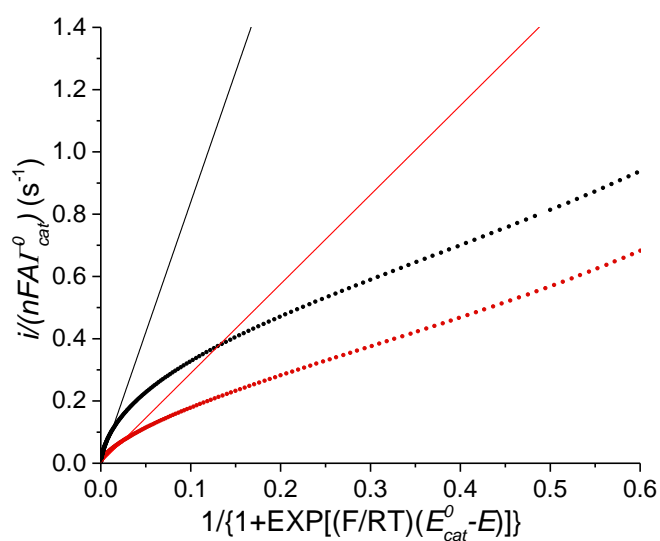


Figure S19. FOWA of anodic direction of CV data for the **Cu-2GH/PAH/phosphate** system (8 deposition cycles) at pH = 10.55 (red) and 10.98 (black). Associated data and conditions are found in Table S2.

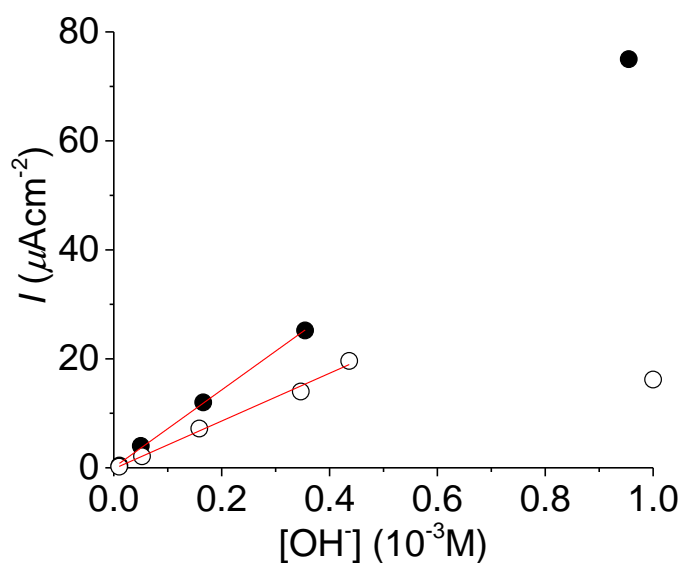


Figure S20. Change in current density with $[\text{OH}^-]$ after electrolysis at 1.1 V vs. Ag/AgCl for 5 min on LbL-ITO electrodes in 0.1 M phosphate electrolyte at various pH values. Open circles stand for **Cu-3G/PLL/phosphate**, full circles for **Cu-2GH/PAH/phosphate**. The corresponding experiments and details are shown in Figs. S5 and S13.